Available online at www.sciencedirect.com

ScienceDirect

Ceramics International 40 (2014) 2023–2028

CERAMICS INTERNATIONAL

www.elsevier.com/locate/ceramint

Structural and magneto-transport properties of $(La_{0.6}Ca_{0.2}Sr_{0.2}MnO_3)_{1-x}$ $(Sb_2O_3/CuO)_x$ composites

M. Nasri[a,*], M. Triki[a], E. Dhahri[a], P. Lachkar[b], E.K. Hlil[c]

[a]Laboratoire de Physique Appliquée, Faculté des Sciences, B.P. 1171, 3000 Sfax, Université de Sfax, Tunisie
[b]MCBT, Institut Néel, CNRS—25 avenue des Martyrs, bâtiment E, BP 166, 38042 Grenoble cedex 9, France
[c]Institut Néel, CNRS—Université J. Fourier, BP 166, 38042 Grenoble, France

Received 22 June 2013; received in revised form 21 July 2013; accepted 23 July 2013
Available online 30 July 2013

Abstract

The $(La_{0.6}Ca_{0.2}Sr_{0.2}MnO_3)_{1-x}(Sb_2O_3/CuO)_x$ ($x=0.00$, 0.03, 0.07, 0.12 and 0.18) composites were prepared by the solid-state reaction technique. $(La_{0.6}Ca_{0.2}Sr_{0.2}MnO_3)_{1-x}(Sb_2O_3/CuO)_x$ are identified by X-ray diffraction and SEM analysis as a two phases consisting of ferromagnetic manganite phase and Sb_2O_3/CuO phase. Magnetic measurement reveals that the Curie temperature as well as the saturation value of magnetization is gradually weakened by Sb_2O_3/CuO addition. The temperature dependence of resistivity shows that the transport behavior of the composites is governed by the grain boundaries. It is suggested that the Sb_2O_3 addition, acts as a separation layer between grains. Whereas, the introduction of CuO into the grain boundaries forms artificial conducting network and improves the carrier to transport. The maximum magnetoresistance was observed to be ≈60% at 10 K for $x=0.03$ which is larger than the largest MR value of pure $La_{0.6}Ca_{0.2}Sr_{0.2}MnO_3$ (40% at 10 K) in a 2 T magnetic field. Enhanced MR effect at a wide temperature range is consistent with the disorder-driven amplification of spin-dependent transport.

Keywords: B. Composite; B. Grain boundaries; Magnetoresistance; Spin dependent transport

1. Introduction

The colossal magnetoresistance (CMR) effect as well as the rich variety of crystallographic, magnetic and electronic properties in mixed valence rare-earth manganese oxides, $Ln_{1-x}A_xMnO_3$ (where Ln=La, Nd, Pr, etc. and A=Ca, Sr, Ba, etc.), has generated renewed interest in the study of these materials [1–7]. The CMR behavior can be understood in the framework of the double exchange (DE) interaction, which considers the transfer of one e_g electron between neighboring ions through the Mn^{3+}–O^{2-}–Mn^{4+} path [8]. In most cases, the CMR phenomenon is often triggered at high magnetic fields and comparatively low temperatures, which hinders its practical applications [9].

Recently, the discovery that grain boundaries and interfaces has attracted remaking interest in these polycrystalline compounds make them attractive for applications usually requiring a large and almost temperature independent magnetoresistance (MR) effect at low applied field. Many research groups have prepared manganite-based composites, where the secondary phases such as Al_2O_3 [10], CeO_2 [11], $SrTiO_3$ [12], and $BaTiO_3$ [13] are assumed to be chemically immiscible with the manganite matrix. In these composites, the increased structural disorder magnetically decouples the neighboring ferromagnetic grains, resulting in a more random distribution of grain magnetization at zero field. The enhanced MR response is achieved when the magnetized grains are aligned in low magnetic field. These experiments clearly show that it is crucial to enhance the spin misorientation for virgin states in order to enhance the MR. Several models have been proposed for theoretical description of grain boundary behaviors in the perovskite manganites. Hwang et al. [14] proposed a model based on spin polarized tunneling between ferromagnetic grains through an insulating grain boundary barrier. However, Guinea [15] pointed out that probably tunneling via paramagnetic impurity states in the grain boundary barrier takes place.

$La_{0.6}Ca_{0.4}MnO_3$ (LCMO) and $La_{0.6}Sr_{0.4}MnO_3$ (LSMO) are two well-studied manganites among the large number of pure CMR materials, whose ferromagnetic–paramagnetic transition

*Corresponding author. Tel.: +216 96 990 194; fax: +216 74 67 66 09.
E-mail address: marianasri@yahoo.fr (M. Nasri).

0272-8842/$ - see front matter © 2013 Elsevier Ltd and Techna Group S.r.l. All rights reserved.
http://dx.doi.org/10.1016/j.ceramint.2013.07.113

temperature (T_C) are 264 K and 372 K, respectively [16]. In the present work, $La_{0.6}Ca_{0.2}Sr_{0.2}MnO_3$ (LCSMO) is selected as the matrix which is a mixture of LCMO and LSMO. Due to the different T_C values of LCMO and LSMO, by mixture the content of Ca and Sr in the composite we can obtain MR within a wide temperature range. The variation of magnetotransport behaviors between conductor-combined and insulator-combined composites will be discussed.

2. Experimental details

The $(LCSMO)_{1-x}(Sb_2O_3/CuO)_x$ ($x=0.00$, 0.03, 0.07, 0.12 and 0.18) composites were prepared by the conventional solid state reaction method in two steps. Firstly, stoichiometric mixtures of La_2O_3, $CaCO_3$, $SrCO_3$ and MnO_2 powders were mixed, ground and then calcined at 900 °C for 24 h. The obtained mixture was reground properly, pressed into the form of pellets and sintered at 1200 °C for 12 h with several periods of grinding and repelleting. Secondly, LCSMO powder was mixed with different fractions of Sb_2O_3/CuO and sintered at 900 °C for 12 h. The phases of samples were examined by X-ray diffraction with CuK_α radiation $\lambda=1.5406$ Å. The data was analyzed by the Rietveld method using the Fullprof program [17]. Magnetic measurements were carried out under using the BS1 magnetometer developed at the Neel Institute. The temperature dependence of resistivity was measured with the standard four probe method in a commercial Physical Property Measurement System (PPMS Quantum Design) under different magnetic applied fields.

3. Results and discussions

Fig. 1 shows the XRD patterns at room temperature for $(LCSMO)_{1-x}(Sb_2O_3/CuO)_x$ and composites. For all combined specimens, the XRD analysis exhibits the existence of two phases: one is related to LCSMO rhombohedral perovskite structure (R-3c space group) with the lattice parameters: $a=b=5.476$ Å and $c=13.279$ Å [16], the other is referring to (Sb_2O_3, CuO) phase. With increasing x content, the relative intensities of diffraction peaks for the LCSMO phase do not shift, whereas, the diffraction peaks corresponding to the second introduced phase appear systematically. It is hard to see the peaks related to CuO phase (only for $x=0.18$) [18]. However, for the Sb_2O_3 phase, peaks can be clearly seen [19]. No extra phase is obtained indicating that the reactions between the LCSMO and Sb_2O_3/CuO are negligible. Sb_2O_3/CuO is probably distributed at the grain boundaries and on the surfaces of LCSMO grains [20,21]. Hence, in the second step of combined sample synthesis, the shorter sintering time could decrease the inter-diffusion between LCSMO and Sb_2O_3/CuO grains.

In order to analyze the effects of the Sb_2O_3/CuO on the microstructure of LCSMO grains and the distribution of the Sb_2O_3/CuO in the composites, the fracture sections of all the samples were examined by the SEM. The typical SEM micrographs of the composites (x=0.00 and 0.18) are indicated in Fig. 2. As shown in Fig. 2(a) an almost clear grain boundary is observed in the pure sample LCSMO ($x=0.00$). However, in the

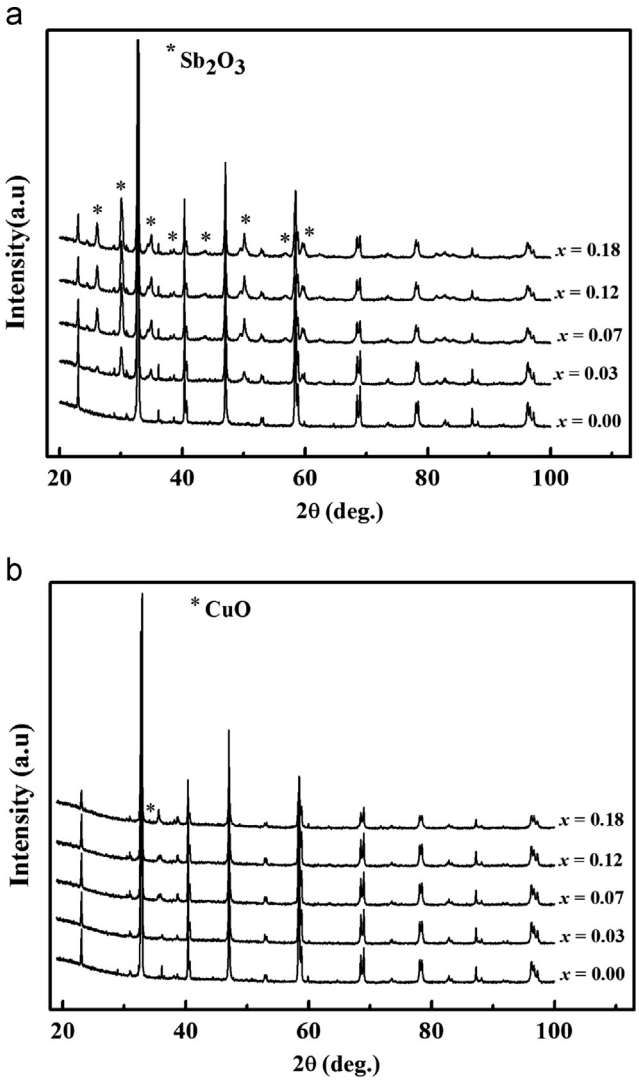

Fig. 1. XRD patterns for $(LCSMO)_{1-x}(Sb_2O_3)_x$ (a) and $(LCSMO)_{1-x}(CuO)_x$ (b) composites at room temperature.

Sb_2O_3/CuO doped composites, the Sb_2O_3/CuO present mainly at the grain boundaries and grain surfaces of LCSMO as shown in Fig. 2(b–c). Thus, as x increases, Sb_2O_3/CuO segregates as a separate phase in the LCSMO matrix, and makes the grain boundaries of the LCSMO ambiguous at high doping level. As x increases, more and more, Sb_2O_3/CuO diffuses from the interior of the LCSMO grains and gets segregated in the grain boundaries.

Fig. 3 shows the thermal magnetization under an applied field of 0.05 T for both series. The Curie temperatures T_C at which dM/dT reaches its extremum are shown in Table 1. The value of saturate magnetization, M_S, which was taken at 5 K, decreases with the concentration of Sb_2O_3/CuO (Fig. 3 (inset)) as reported in Refs. [22,23]. Thereby, the embedding of Sb_2O_3/CuO into LCSMO matrices dilutes the magnetization of the composite samples. Indeed, the secondary phase segregates into the grain boundaries or interfacial region which leads to the suppression of the DE interaction returns to the decrease of the ferromagnetic alignment of Mn ions in neighboring LCSMO grains, because the second introduced phase at the grain boundaries blocks the alignment of Mn ions in neighboring pure LCSMO grains.

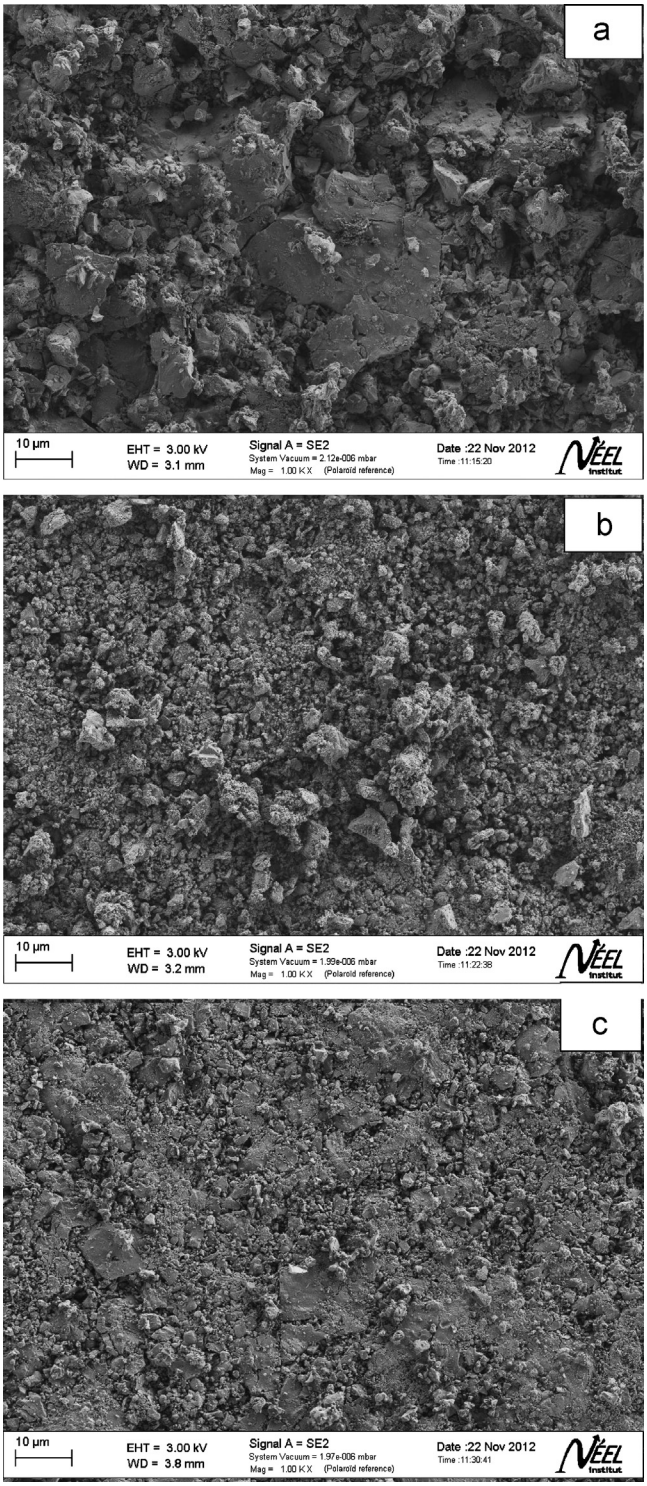

Fig. 2. SEM micrographs for x=0.00 (a), x=0.18 Sb_2O_3 (b) and x=0.18 CuO (c).

Consequently, a lowering of the transition temperature T_C with the increase in x content is observed indicating that magnetic spin disorder is induced by the grain boundaries in the composites [20,21].

The temperature dependence of resistivity for $(LCSMO)_{1-x}(Sb_2O_3/CuO)_x$ composites was measured under the applied magnetic fields of zero and 2 T. Fig. 4 shows the plots of

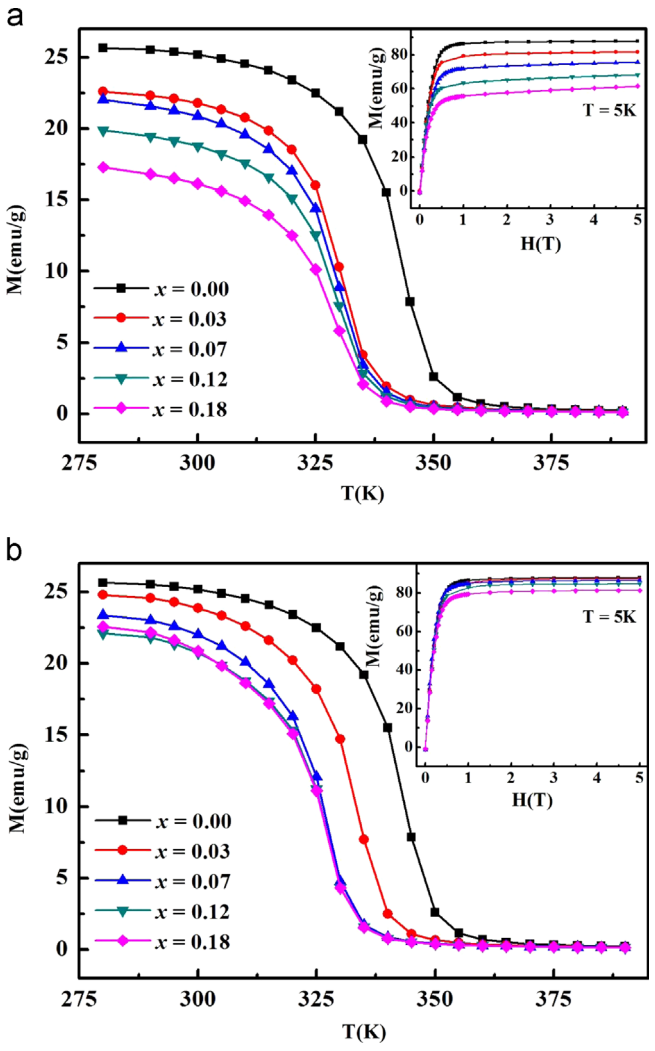

Fig. 3. Temperature dependence of magnetization at 0.05 T for $(LCSMO)_{1-x}(Sb_2O_3)_x$ (a) and $(LCSMO)_{1-x}(CuO)_x$ (b) composites. Inset: field dependence of magnetization at 5 K.

resistivity versus temperature in zero applied magnetic field. All the composites have a resistivity peak at T_ρ. The lower T_ρ than T_C is a remarkable feature of extrinsic transport behavior, which indicates the important role of grain boundary effect in the transport behavior [24,25]. The variation of T_ρ with field and x content is reported in Table 2. T_ρ of the composites shifts towards lower temperatures with increasing Sb_2O_3, which can be explained from the parallel resistor network model [26]. The introduction of Sb_2O_3 depresses metallic conduction by blocking conduction channels at grain boundaries between LCSMO grains, leading to a decrease of T_ρ. With increasing Sb_2O_3 doping level x, the high resistivity of the composites should be related to the effect of insulator phase Sb_2O_3. In pure LCSMO, electrical transport occurs through a direct contact among LCSMO grains. However, there are two conduction channels in LCSMO/Sb_2O_3 composites, which is similar to another group report [10,27]. One is related to the LCSMO grains, the other is related to Sb_2O_3 at the grain boundaries or surfaces of the LCSMO grains, showing energy barriers to the electrical transport process. In addition, the Sb_2O_3 grains will cause magnetic disorder and contamination at the grain boundaries of LCSMO, inducing

Table 1
Ferromagnetic to paramagnetic transition temperatures of $(LCSMO)_{1-x}(Sb_2O_3/CuO)_x$ composites.

$(1-x)$LCSMO/$x$$Sb_2O_3$	x=0.00	x=0.03	x=0.07	x=0.12	x=0.18
T_C	345	335	325	325	325
$(1-x)$LCSMO/xCuO	x=0.00	x=0.03	x=0.07	x=0.12	x=0.18
T_C	345	330	329	328	326

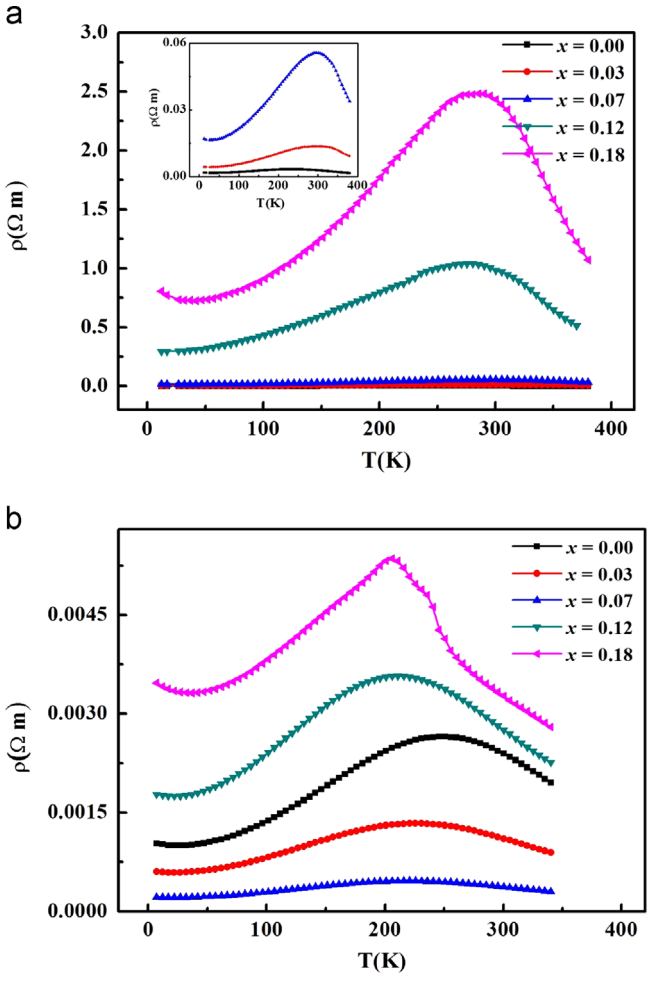

Fig. 4. Temperature dependence of resistivity for $(LCSMO)_{1-x}(Sb_2O_3)_x$ (a) and $(LCSMO)_{1-x}(CuO)_x$ (b) composites measured at 0 T.

inhibition of the metallic conduction. So the more Sb_2O_3 segregates at the grain boundaries of LCSMO, the more the influence on the conduction and the resistivity of the composites increases. Since the electrons are almost completely polarized inside a magnetic domain in pure LCSMO, electrons easily transferred between Mn^{3+} and Mn^{4+} ions. However, when these electrons travel across grains, strong spin-dependent scattering at the boundaries leads to a high resistivity. For x=0.03, the admixture of non-magnetic and insulating Sb_2O_3 separates slightly the FM metallic clusters and as the Sb_2O_3 concentration increases the spatial separation of these grains/clusters further increases. In other terms, at low addition rates, more LCSMO grains connect directly when compared to those with higher x content and the composites exhibit transport behavior similar to pure LCSMO. Similar result was also reported in $La_{2/3}Ca_{1/3}MnO_3$ for x=0.09 [28]. Nevertheless, as Sb_2O_3 is distributed at the grain boundaries of LCSMO, it enhances the disorder of the Mn ions spin orientation between the grain boundaries and reduces the ferromagnetic coupling which leads to the decrease of T_ρ with increasing x content.

Conversely, it is found that the presence of CuO in LCSMO matrices results in a lowering of the transition temperature; the downward shift of T_ρ is sharply at low CuO level and then becomes gradual with further increase of x. According to the mechanism of spin-polarized tunneling, the transition to metallic behavior occurs only when the neighboring grain moments correlate with FM one. Spin disorder at the grain boundaries affect ferromagnetic coupling of LCSMO grain moments, which result in the lowering of T_ρ. The decrease of peak resistivity for $x<0.12$ can be explained by two facts: firstly, the oxygen liberated from the breaking of Cu–O bond is likely to move inside the grains, compensating the oxygen loss there, if any, by filling the oxygen vacancy in the bond between Mn^{3+} and Mn^{4+} ions. This would make the electron transfer easier, resulting in the decrease of the electrical resistivity. Secondly, the existence of conductive metal Cu among the LCSMO grains make the grain boundary more conducting, which opens a new conducting channels among the LCSMO grains, leading to the decrease in the spin dependant scattering [29]. Similar results were observed in Refs. [30,31]. At the range of $x>0.12$, the distribution of the CuO phase forms barriers that encompass LCSMO completely, the mobility of charges carriers and the number of hopping sites are reduced [32]. Thus, the volume fraction of the ferromagnetic LCSMO phase decreases and the resistivity of the composites increases.

Fig. 5 presents the MR characteristics under an applied field of 2 T. Here, MR is defined as $(\rho_0-\rho_H/\rho_0\times 100)$, where ρ_0 and ρ_H stand for the resistivity at 0 and H applied field, respectively. The maximum MR was observed to be ≈60% at 10 K and ≈35% at 300 K for x=0.03 (Sb_2O_3/CuO) respectively, which are larger than those of pure $La_{0.6}Ca_{0.2}Sr_{0.2}MnO_3$ (40% at 10 K and 12% at 300 K). The enhancement MR originates from the spin dependent tunneling and the scattering process at the interfaces of the grains [33–36]. At the surfaces of LCSMO grains, strong magnetic scattering of polarized charge carriers whose strength is field dependent, increased with (Sb_2O_3/CuO) addition. Application of a moderate field can align the magnetic domains associated with the grains into a parallel configuration due to the suppression of the scattering causing an enhancement of MR [37,38]. With further increase of doping content, the grain boundaries become too thick for the spin preserving electron tunneling and it is difficult for the applied field to align the domain along the field direction which

Table 2
Metal–insulator transition temperatures of $(LCSMO)_{1-x}(Sb_2O_3/CuO)_x$ composites.

	$x=0.00$	$x=0.03$	$x=0.07$	$x=0.12$	$x=0.18$
$(1-x)LCSMO/xSb_2O_3$					
Magn. field 0 T	232	300	290	283	278
Magn. field 2 T	235	302	292	285	283
Magn. field 5 T	249	305	295	287	285
$(1-x)LCSMO/xCuO$					
Magn. field 0 T	232	210	200	193	189
Magn. field 2 T	235	219	213	208	205
Magn. field 5 T	249	225	220	210	207

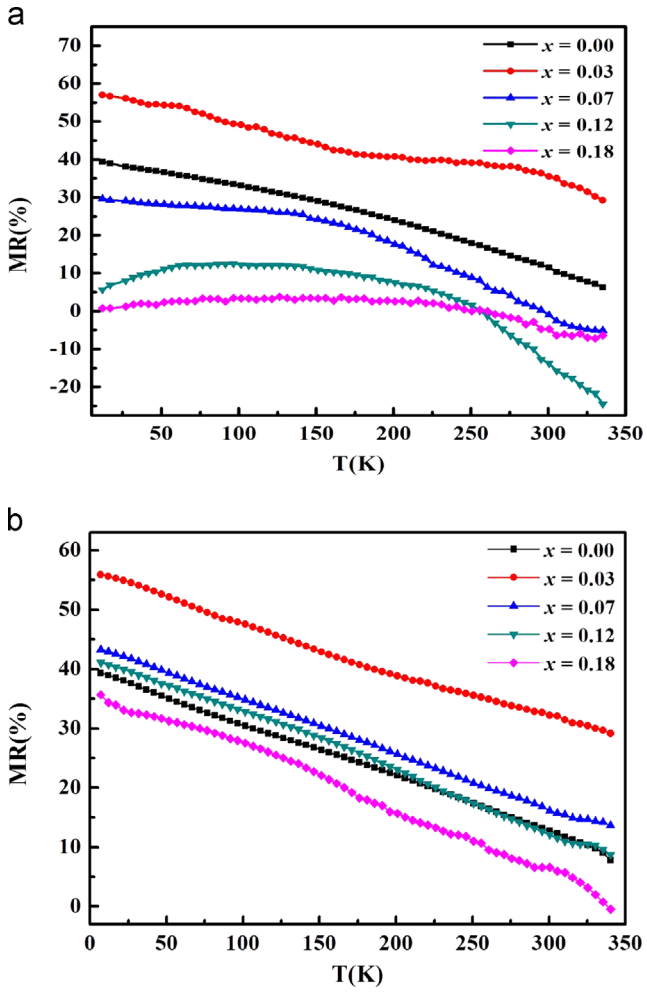

Fig. 5. Magnetoresistance versus temperature for $(LCSMO)_{1-x}/(Sb_2O_3)_x$ (a) and $(LCSMO)_{1-x}/(CuO)_x$ (b) composites.

induces the decrease of the MR effects. It is interesting to see that MR remained almost independent of temperature over a wide range of temperature. Such a behavior of MR is very important from the application point of view [39].

4. Conclusion

We have investigated the structural, magnetic and magneto-transport properties of Sb_2O_3/CuO doped LCSMO composites. The XRD and SEM results show that Sb_2O_3/CuO is not imbedded into the lattice of LCSMO grains and is found to remain in surfaces and grain boundary regions. The observed decrease of both the Curie temperature and the saturation magnetization values are attributed to the effect of magnetic disorder. We demonstrated that the enhanced MR is related to the enhanced spin-dependent transport at the surfaces between LCSMO grains; MR response can be improved by diluting the system and by an increase in the interfacial disorder.

Acknowledgments

This work is supported by the Tunisian National Ministry of Higher Education, Scientific Research and the French Ministry of Higher Education and Research of CMCU 10G1117 collaboration, within the frame work of collaboration Franco-Tunisian.

References

[1] R.M. Kusters, J. Singleton, D.A. Keen, R. McGreevy, W. Hayes, Physica B 155 (1989) 362.
[2] R. von. Helmolt, J. Wecker, B. Holzapfel, L. Schultz, K. Samwer, Physical Review Letters 71 (1993) 2331.
[3] R.M. Thomas, V. Skumryev, J.M.D. Coey, S. Wirth, Journal of Applied Physics 85 (1999) 5384.
[4] M. Bejar, R. Dhahri, F. El Halouani, E. Dhahri, Journal of Alloys and Compounds 414 (2006) 31.
[5] J.J. Neumeier, J.L. Cohn, Physical Review B 61 (2000) 14319.
[6] S. Othmani, M. Bejar, E. Dhahri, E.K. Hlil, Journal of Alloys and Compounds 475 (2009) 46.
[7] S. Roy, N. Ali, Journal of Applied Physics 89 (2001) 7425.
[8] C. Zener, Physical Review 82 (1951) 403.
[9] J.S. Park, C.O. Kim, Y.P. Lee, V.G. Prokhorov, G.G. Kaminsky, V.A. Komashko, H.C. Ri, Journal of the Korean Physical Society 42 (2003) L309.
[10] L.E. Hueso, J. Rivas, Journal of Applied Physics 89 (2001) 1746.
[11] L.I. Balcells, A.E. Carrillo, B. Martinez, J. Fontcuberta, Applied Physics Letters 74 (1999) 4.
[12] D.K. Petrov, L.K. Elbaum, J.Z. Suan, C. Field, P.R. Duncombe, Applied Physics Letters 75 (1999) 995.
[13] M. Triki, R. Dhahri, M. Bekri, E. Dhahri, M.A. Valente, Journal of Alloys and Compounds 509 (2011) 9460.
[14] H.Y. Hwang, S.W. Cheong, N.P. Ong, B. Batlogg, Physical Review Letters 77 (1996) 2041.
[15] F. Guinea, Physical Review B 58 (1998) 9212.

[16] M. Nasri, M. Triki, E. Dhahri, E.K. Hlil, Journal of Alloys and Compounds 546 (2013) 84.
[17] J. Rodriguez-Carjaval, FULLPROF'98, Laboratoire Leon Briouillon (CEA-CNRS), 1998.
[18] M. Juhong, Y. Songliu, R. Guangming, X. Xun, Y. Gongqi, Journal of Rare Earths 25 (2007) 204.
[19] J.H. Miao, S.L. Yuan, G.M. Ren, X. Xiao, G.Q. Yu, Y.Q. Wang, S.Y. Yin, Material Science and Engineering B 136 (2007) 67.
[20] C.S. Xiong, Y. Zeng, Y.H. Xiong, J. Zhang, Y.B. Pi, L. Zhang, J. Xiong, X.W. Cheng, F.F. Wei, L.J. Li, Physica B 403 (2008) 3266.
[21] C.S. Xiong, Y.F. Cui, Y.H. Xiong, H.L. Pi, X.C. Bao, Q.P. Huang, Y. Zeng, F.F. Wei, C.F. Zheng, J. Zhu, Journal of Solid State Chemistry 181 (2008) 2123.
[22] A. Gaur, G.D. Varma, Solid State Communications 139 (2006) 310.
[23] S.L. Young, C.C. Lin, J.B. Shi, H.Z. Chen, L. Horng, Materials Letters 60 (2006) 1682.
[24] H.Y. Hwang, Z.G. Xu, C.H. Yan, Z.M. Wang, T. Zhu, C.S. Liao, S. Gao, Z.X. Xu, Solid State Communications 114 (2000) 43.
[25] Y.L. Fu, Applied Physics Letters 77 (2000) 118.
[26] A.D. Andres, M. Garcia-Hernandez, J.L. Martinez, Physical Review B 60 (1999) 7328.
[27] D. Das, C.M. Srivastava, D. Bahadur, A.K. Nigam, S.K. Malik, Journal of Physics: Condensed Matter 16 (2004) 4089.
[28] L. Gao, L. Bai, C. Li, X. Liu, Z. Wu, D. Zheng, Y. Lu, Journal of Alloys and Compounds 522 (2012) 25.
[29] A. Gupta, J.Z. Sun, Journal of Magnetism and Magnetic Materials 200 (1999) 24.
[30] J.H. Miao, S.L. Yuan, G.M. Ren, X. Xiao, G.Q. Yu, Journal of Rare Earths 25 (2007) 204.
[31] J.H. Miao, S.L. Yuan, L. Yuan, G.M. Ren, X. Xiao, G.Q. Yu, Y.Q. Wang, S.Y. Yin, Journal of Materials Research Bulletin 43 (2008) 631.
[32] J.R. Sun, G.H. Rao, Y.Z. Zhang, Applied Physics Letters 72 (1998) 3208.
[33] H. Kim, J. Dho, S. Lee, Physical Review B 62 (2000) 5674.
[34] S.L. Ye, W.H. Song, J.M. Dai, K.Y. Wang, S.G. Wang, J.J. Du, Journal of Applied Physics 90 (2001) 2943.
[35] Z.G. Huang, Z.G. Chen, K. Peng, D. Wang, F. Zhang, W. Zhang, Y. Du, Physical Review B 69 (2004) 094420.
[36] R.Q. Gai, Z.G. Huang, S.Y. Chen, Y.W. Du, Transactions of Nonferrous Metals Society of China 15 (2005) 323.
[37] G. Anurag, G.D. Varma, Solid State Communications 139 (2006) 310.
[38] C.H. Yan, Z.G. Xu, T. Zhu, Z.M. Wang, F.X. Cheng, Y.H. Huang, C.S. Liao, Journal of Applied Physics 87 (2000) 5588.
[39] T. Wang, X. Chen, F. Wang, W. Shi, Physica B 405 (2010) 3088.